

# Effect of Sintering Temperature on Structural and Morphological Properties of Mn-Substituted Lithium Ferrite

Rajendra P. Patil,\* Prashant N. Nikam, Sarjerao B. Patil, Ramdas K. Dhokale, Vijay S. Sawant, and Satish B. Shelke

Manganese-substituted lithium ferrite is synthesized by sol-gel method. The sample is sintered at different temperatures in air. Their structural and morphological properties are studied by X-ray diffraction, scanning electron microscopy, and FT-IR techniques. The X-ray diffraction patterns reveal that all the samples consist of nanocrystalline single cubic phase structure. The morphological studies of synthesized nanocrystalline samples are obtained from the scanning electron microscopy technique. It can be seen that, the average grain size is increased significantly with increasing the sintering temperature. FT-IR studies indicate that the spinel phase formation takes place at higher sintering temperature.

Lithium ferrites have been studied and developed for many years because of their structural, electrical, and magnetic properties that provide better applications of scientific and technological interest.<sup>[13–17]</sup> Lithium ferrite in the spinel phase,  $\text{Li}_{0.5}\text{Fe}_{2.5}\text{O}_4$ , has a square hysteresis loop, high magnetization, and high Curie temperature. These properties are useful for technological applications such as the development of low-cost materials microwave devices. Many transition metal cations such as Mn, Cr, Co, and Ti can be introduced into the lattice of the magnetic structure, which is useful to various applications.<sup>[18–21]</sup>

## 1. Introduction

Ferrospinel are widely used in many important components such as microwave devices, magnetic devices, transformer cores, choke coils, high-frequency instruments, data storage, noise filters, and recording heads, as a ferrofluids and catalytic activity due to the interesting physicochemical properties.<sup>[1–3]</sup> These properties are dependent on the nature of ions and their charge distribution among tetrahedral and octahedral sites. The modifications of the structural and magnetic properties of ferrites are due to substitution of different ions and have been studied by various workers.<sup>[4–12]</sup>

Literature survey shows that there are no reports on effect of sintering temperature on structural and morphological properties of manganese-substituted lithium ferrite prepared by sol-gel method. Sol-gel method is a useful technique as compared to other methods, due to the better homogeneity, smaller particle size, and modification of surface area. The sol-gel autocombustion technique is an effective method for the synthesis of the mixed-metal oxides. In present investigation, an attempt is made to prepare manganese-substituted lithium ferrite, by sol-gel route.

## 2. Experimental Section

### 2.1. Synthesis Technique

Polycrystalline sample having the general formula,  $\text{Li}_{0.5}\text{Fe}_{1.5}\text{Mn}_{1.0}\text{O}_4$  was synthesized by sol-gel method as shown in Figure 1. High-purity AR-grade ferric nitrate, manganese nitrate, lithium nitrate, and citric acid were used for synthesis. The metal nitrate solutions were mixed in the required stoichiometric ratios in minimum quantity of distilled water. The pH of the solution was maintained between 9 and 9.5 using ammonia solution. The solution mixture was slowly heated around 373 K with constant stirring to obtain a fluffy mass. The precursor powder was sintered at 873 and 973 K for 8 h, then mixed with 2% polyvinyl alcohol as a binder, and uniaxially pressed at a pressure of 8 ton  $\text{cm}^{-2}$  to form the pellets.

### 2.2. Characterization Techniques

Thermal analysis of the different compositions of the unsintered Mn-substituted lithium ferrite sample was carried out from the

R. P. Patil  
Department of Chemistry  
M.H. Shinde Mahavidyalaya  
Affiliated to Shivaji University  
Kolhapur, Maharashtra, India  
E-mail: patilraj\_2005@rediffmail.com

P. N. Nikam, S. B. Patil  
Department of Physics  
Krantisinh Nana Patil College Walwa  
Sangli, Maharashtra, India

R. K. Dhokale  
Department of Chemistry  
Arts, Science and Commerce College  
Naldurg, Maharashtra, India

V. S. Sawant  
Department of Botany  
Arts, Science and Commerce College  
Naldurg, Maharashtra, India

S. B. Shelke  
Department of Physics  
Shri Madhavrao Patil Mahavidyalaya  
Murum, Maharashtra, India

DOI: 10.1002/masy.202000173

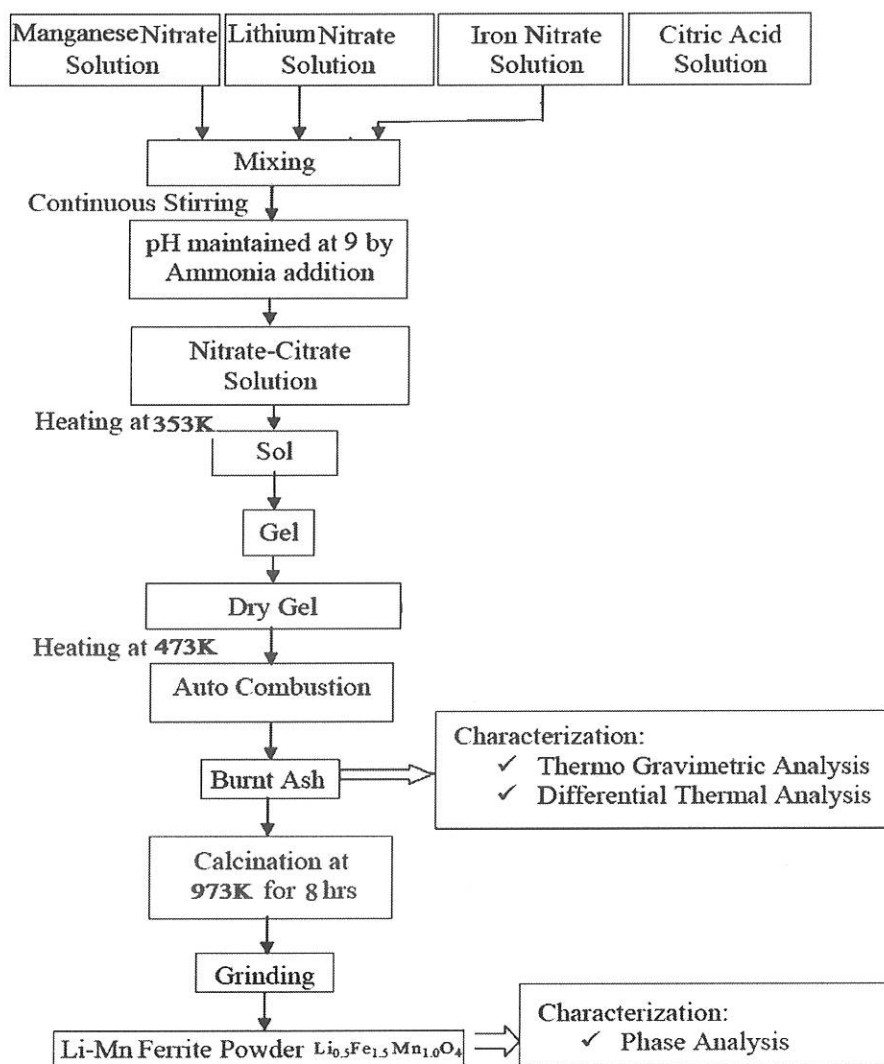


Figure 1. Flow diagram for sol-gel autocombustion technique.

curves of TG-DTA. Stability of the dry citrate complexes was checked by scanning the thermogram in the temperature range of 10–1000°C in static air at the flow rate of 10°C min<sup>-1</sup>. Different kinds of thermodynamic and kinetic parameters were determined from the plots of TG-DTA curves.

The phase formation of the sintered samples was confirmed by x-ray diffraction studies using a Philips PW-1710 x-ray diffractometer with CrK $\alpha$  radiation ( $\lambda = 2.2897 \text{ \AA}$ ) in a  $\theta$ - $2\theta$  geometry at standard atmospheric conditions. The lattice constant was calculated for the cubic phase using following relation.

$$a = d(h^2 + k^2 + l^2)^{\frac{1}{2}} \quad (1)$$

where,

$a$  = Lattice constant,  $(hkl)$  = Miller indices

$d$  = interplanar distance

The crystallite size of sintered samples was calculated from the full width at half maxima of the most intense (311) peak by using Scherrer's formula.

$$t = 0.9\lambda / \beta \cos \theta \quad (2)$$

Where, symbols have their usual meaning.

The X-ray density was calculated according to the formula

$$dx = 8M / Na^3 \quad (3)$$

where,

$N$  = Avagadros number ( $6.023 \times 10^{23}$  atom/mole)

$M$  = Molecular weight, and

$a$  = lattice constant which was calculated from the X-ray diffraction pattern.

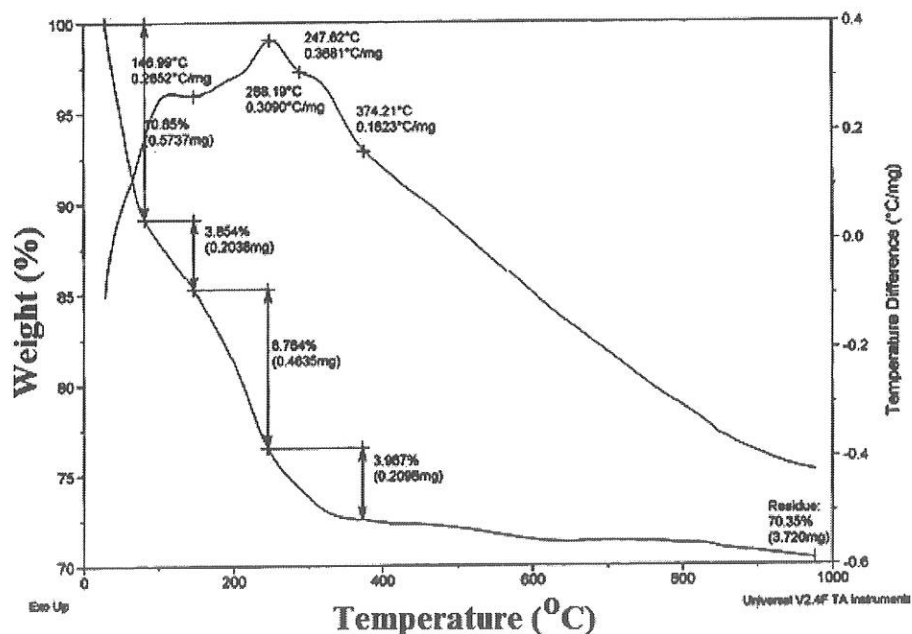


Figure 2. TGA-DTA Spectrum for  $\text{Li}_{0.5}\text{Fe}_{1.5}\text{Mn}_{1.0}\text{O}_4$ .

The FT-IR spectra were recorded in the range of 400–1000  $\text{cm}^{-1}$  on instrument Perkin Elmer-IR spectrophotometer (Model E-2829) in KBr pellets.

The SEM micrograph of the samples was obtained using scanning electron microscope (JEOL-JSM 6360).

### 3. Results and Discussion

#### 3.1. Thermogravimetric Analysis

TG and DTA curves for the dried sample of  $\text{Li}_{0.5}\text{Fe}_{1.5}\text{Mn}_{1.0}\text{O}_4$  sample is presented in Figure 2. As shown in the figure, in the TG curve, the percent weight loss with the temperature is observed. A continuous weight loss was observed from TG curve upto 600°C of the sample in the formation of stable oxide compound. However, DTA curves show one exothermic peak around 290°C. At this temperature, a decomposition of mixed-metal citrate complexes by fragmentation and thermal degradation of organic content occur and this results in the formation of stable mixed-metal oxide.

#### 3.2. X-ray Diffraction Study

X-ray powder diffraction patterns of  $\text{Li}_{0.5}\text{Fe}_{1.5}\text{Mn}_{1.0}\text{O}_4$  sample sintered at different sintering temperature such as 873 and 973 K temperatures are shown in Figure 3. X-ray diffraction data reveal that, the cubic crystalline phase is observed at 973 K. On increasing the sintering temperature, the diffraction peaks become narrower and sharper, suggesting the increase in crystallinity of the samples. The data on lattice constant (a), X-ray density (dx), crystallite size (t) for the samples manganese-substituted lithium ferrite is given in Table 1.

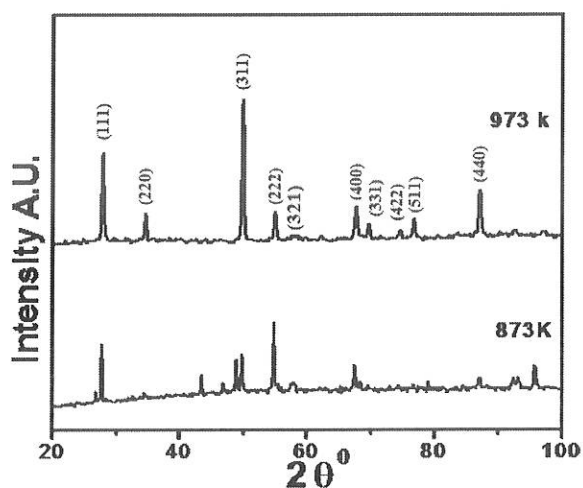


Figure 3. X-ray analysis study for  $\text{Li}_{0.5}\text{Fe}_{1.5}\text{Mn}_{1.0}\text{O}_4$  sample at different sintering temperature.

Table 1. Data on lattice parameter, crystallite size, X-ray density of  $\text{Li}_{0.5}\text{Fe}_{1.5}\text{Mn}_{1.0}\text{O}_4$  sample.

Sintering temperature	Lattice constant (a) [Å]	Crystallite size (t) [nm]	X-ray density(dx) [ $\text{g cm}^{-3}$ ]
873 K	8.29	31.22	4.61
973 K	8.33	32.37	4.74

#### 3.3. Scanning Electron Microscopy

The particle surface morphology was studied using scanning electron microscopy technique (JEOL-JSM 6360 Microscope).

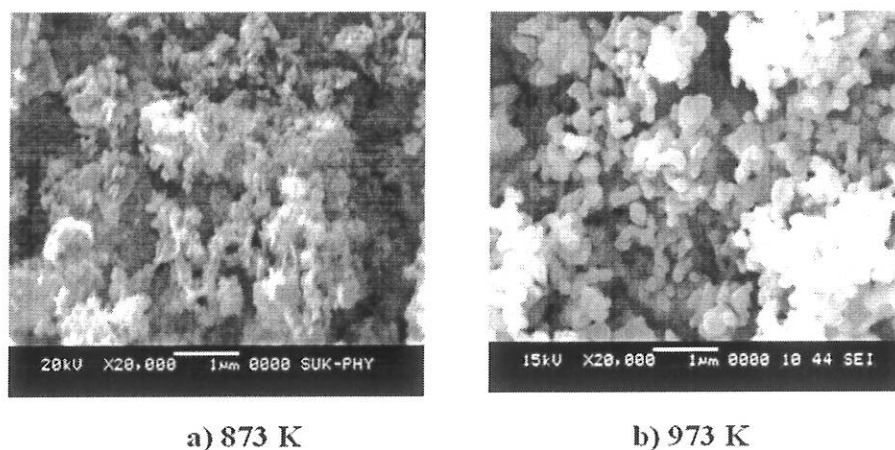


Figure 4. SEM analysis for  $\text{Li}_{0.5}\text{Fe}_{1.5}\text{Mn}_{1.0}\text{O}_4$  sample at different sintering temperature.

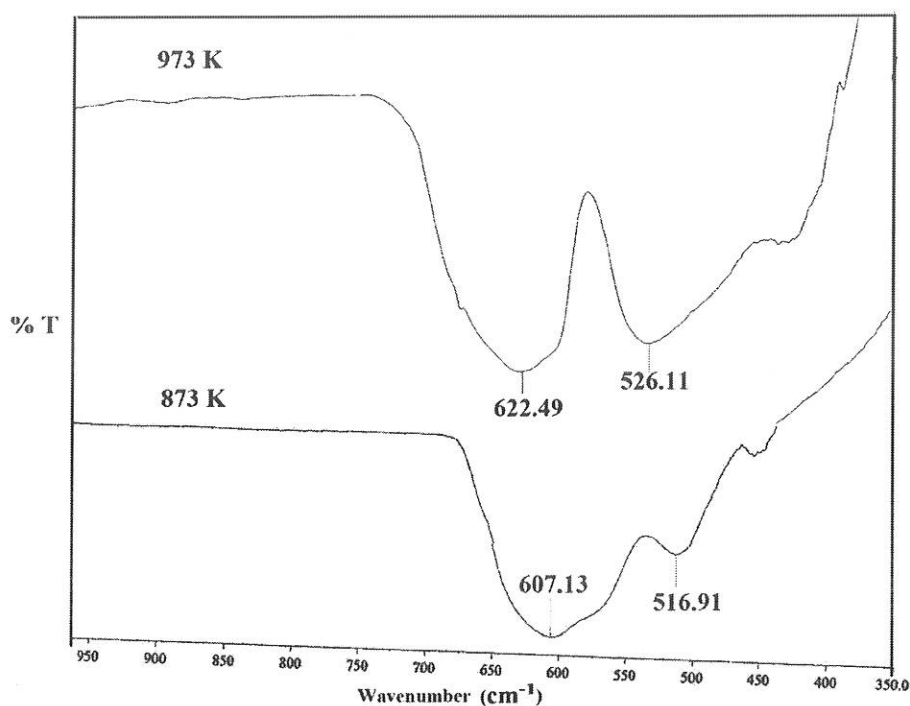


Figure 5. FT-IR spectra for  $\text{Li}_{0.5}\text{Fe}_{1.5}\text{Mn}_{1.0}\text{O}_4$  sample at different sintering temperature.

The microstructure of the samples depends on the sintering temperature and substitution of manganese. The scanning electron micrographs of sintered samples at different temperatures 873 and 973 K are shown in Figure 4. It can be seen that, the average grain size and crystallinity is increased significantly with increasing the sintering temperature and the particle size becomes more uniform at higher sintering temperature. At the sintering temperature of 973 K, substantial grain growth occurs in which the ferrite grains are cubic and well crystalline in nature.

### 3.4. Fourier Transforms Infra-Red Spectroscopy

The FT-IR spectra of all different sintered compositions are shown in Figure 5. Waldron et al. have observed that in normal ferrite, both the absorption bands depend on the nature of octahedral M-O stretching vibration and nature of tetrahedral M-O stretching vibration.<sup>[22]</sup> Earlier study of the vibrational spectra of ferrites a band around 600  $\text{cm}^{-1}$  is attributed to the intrinsic vibrations of tetrahedral complexes and another band around 400  $\text{cm}^{-1}$  is attributed to that of octahedral complexes



(Table 2). The FTIR spectrum of all sintered compositions reveals that the sharp bands appear at higher sintering temperature. It is well known that the vibrational frequencies depend on the cation mass, cation-oxygen bonding force, and distance and unit cell parameter. These bands are mainly dependent on Fe—O distances.<sup>[23]</sup> It is revealed that in normal spinel ferrites, both the bands depend on the nature of octahedral cations while to a lesser extent on tetrahedral ones. It is also observed that the frequency of the absorption bands increases with increase in unit cell volume.

#### 4. Conclusion

$\text{Li}_{0.5}\text{Fe}_{1.5}\text{Mn}_{1.0}\text{O}_4$  sample is successfully synthesized via a sol-gel autocombustion technique. This method is cost-effective and environmentally friendly because of no by-product effluents. X-ray diffraction patterns reveal the broadening of major peaks and are indication of spinel phase formation at 973 K. These data reveal that such sintering temperature for  $\text{Li}_{0.5}\text{Fe}_{1.5}\text{Mn}_{1.0}\text{O}_4$  was as compared to previous studied synthesis method. The effect of the sintering temperature on its grain morphology and microstructure of the samples is studied using SEM method. The FT-IR study indicates that, the spinel phase formation occurs at higher sintering temperature.

#### Acknowledgements

Author (R.P. Patil) is thankful to Shivaji University, Kolhapur, for financial assistance through minor research project under Research Initiation Scheme. Authors are thankful to Prof. P. P. Hankare for his help in experiments and for the valuable discussion.

#### Conflict of Interest

The authors declare no conflict of interest.

#### Keywords

lithium manganese ferrite, scanning electron micrograph, sintering temperature, sol-gel method, x-ray diffraction

- [1] M. L. S. Teo, L. B. Kong, Z. W. Li, G. Q. Lin, Y. B. Gan, *J. Alloys Compd.* **2008**, 459, 557.
- [2] G. Blasse, *Philips Res. Rept.* **1965**, 20, 528.
- [3] J. B. Goodenough, *Mag. and Chem. Bond*, John Wiley, New York, **1966**.
- [4] P. P. Hankare, U. B. Sankpal, R. P. Patil, P. D. Lokhande, R. Sasikala, *Mater. Sci. Eng.: B.* **2011**, 176, 103.
- [5] P. P. Hankare, R. P. Patil, K. M. Garadkar, R. Sasikala, B. K. Chougule, *Mater. Res. Bull.* **2011**, 46, 447.
- [6] P. P. Hankare, R. P. Patil, U. B. Sankpal, S. D. Jadhav, K. M. Garadkar, S. N. Achary, *J. Alloy. Compd.* **2011**, 509, 276.
- [7] J. B. Goodenough, A. L. Loeb, *Phys. Rev.* **1955**, 98, 391.
- [8] A. P. B. Sinha, N. R. Sanjana, A. B. Biswas, *Acta Cryst.* **1957**, 10, 439.
- [9] P. Nathawani, V. S. Darshane, *J. Phys. C: Solid State Phys.* **1988**, 21, 3191.
- [10] G. R. Dube, V. S. Darshane, *Bull. Chem. Soc. Jpn* **1991**, 64, 2449.
- [11] S. C. Watawe, U. A. Bamne, S. P. Gonbare, R. B. Tangsali, *Mater. Chem. Phys.* **2007**, 103, 323.
- [12] S. Singhal, S. K. Barthwal, K. Chandra, *Indian J. Pure Appl. Phys.* **2007**, 45, 821.
- [13] N. Ramachandran, A. B. Biswas, *J. Solid State Chem.* **1979**, 30, 61.
- [14] T. Shirane, R. Kanno, Y. Kawamoto, Y. Takeda, M. Takano, T. Kamiyama, F. Izumi, *Solid State Ionics* **1995**, 79, 227.
- [15] M. Tabuchi, *J. Solid State Chem.* **1998**, 141, 554.
- [16] J. Smit, H. P. J. Wijn, *Ferrites*, Wiley, New York **1959**, p. 158.
- [17] H. Igarashi, K. Okazaki, *J. Am. Ceram. Soc.* **1977**, 60, 51.
- [18] A. B. Gadkari, T. J. Shinde, P. N. Vasambekar, *Mater. Chem. Phys.* **2009**, 114, 505.
- [19] G. M. Argentina, P. D. Baba, *IEEE Trans. Microw. Theory Tech.* **1974**, 22, 652.
- [20] P. P. Hankare, R. P. Patil, U. B. Sankpal, S. D. Jadhav, P. D. Lokhande, K. M. Jadhav, R. Sasikala, *J. Solid State Chem.* **2009**, 182, 3217.
- [21] P. P. Hankare, R. P. Patil, U. B. Sankpal, S. D. Jadhav, I. S. Mulla, K. M. Jadhav, B. K. Chougule, *J. Magn. Magn. Mater.* **2009**, 321, 3270.
- [22] R. D. Waldron, *Phys. Rev.* **1955**, 99, 1727.
- [23] R. P. Patil, P. P. Hankare, K. M. Garadkar, R. Sasikala, *J. Alloy. Compd.* **2012**, 523, 66.

  
**PRINCIPAL**  
Arts Science & Commerce College  
Naldurg, Dist. Osmanabad-413602